Supporting Information File

Probing through-space and through-bond magnetic exchange couplings in a new benzotriazinyl radical and its metal complexes

Rajendar Nasani,[‡a] Thulaseedharan Nair Sailaja Sidharth,[§‡a] Subhadip Roy,[a] Arpan Mondal,[a] Jeremy M. Rawson,*[b] and Sanjit Konar*[a]

[a] Department of Chemistry, Indian Institute of Science Education and Research Bhopal, Bhopal Bypass Road, Bhauri, Bhopal 462 066, India. E-mail: skonar@iiserb.ac.in; Fax: +91-755-6692392; Tel: +91-755-6692339.

[b] Department of Chemistry & Biochemistry, The University of Windsor, 401 Sunset Ave., Windsor, ON, CANADA, N9B 3P4; E-mail: jmrawson@uwindsor.ca

[‡]Both the authors have equal contribution to this work.

[§]Undergraduate Researcher.

S.1 Cyclic voltammetry

Electrochemical experiments were carried out on a CH Instruments (Model 760D) potentiostat with scans of 100 mV/s on solutions of **Rad$_2$** in dichloromethane containing 0.1 M (^{n}Bu$_4$N][PF$_6$] supporting electrolyte at 25°C. The three electrode electrochemical cell consisted of a glassy carbon working electrode, a Pt wire counter electrode, and an Ag/AgNO$_3$ (10 mM AgNO$_3$ in MeCN) non-aqueous reference electrode.

The redox behaviour of **Rad$_2$** exhibits two fully reversible waves that correspond to the $-1/0$ and $0/+1$ processes (Figure S1). Oxidation of **Rad$_2$** occurred at +0.31 V versus ferrocene/ferrocenium, whereas the corresponding reduction potential occurred at -0.85 V, respectively.
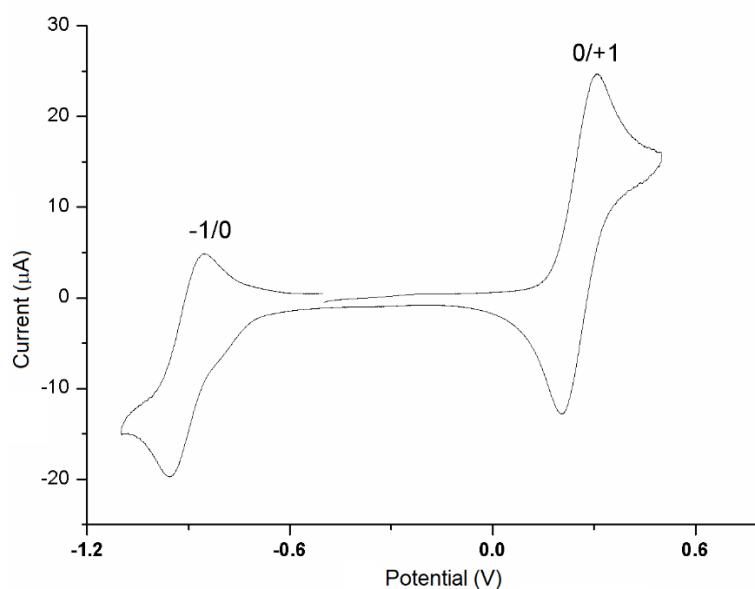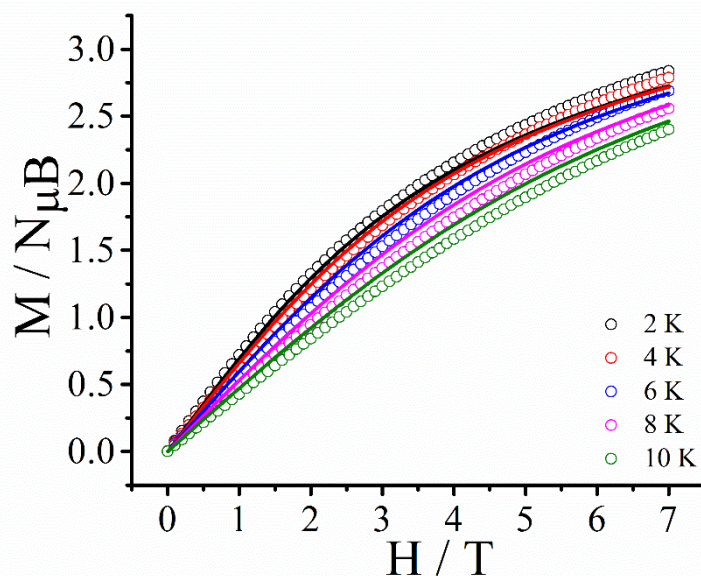

Figure S1. Cyclic voltammogram of **Rad$_2$** in CH$_2$Cl$_2$ using [^{n}Bu$_4$N][PF$_6$] supporting electrolyte. Scan rate 100 mV/s (Reference Ag/Ag$^+$).
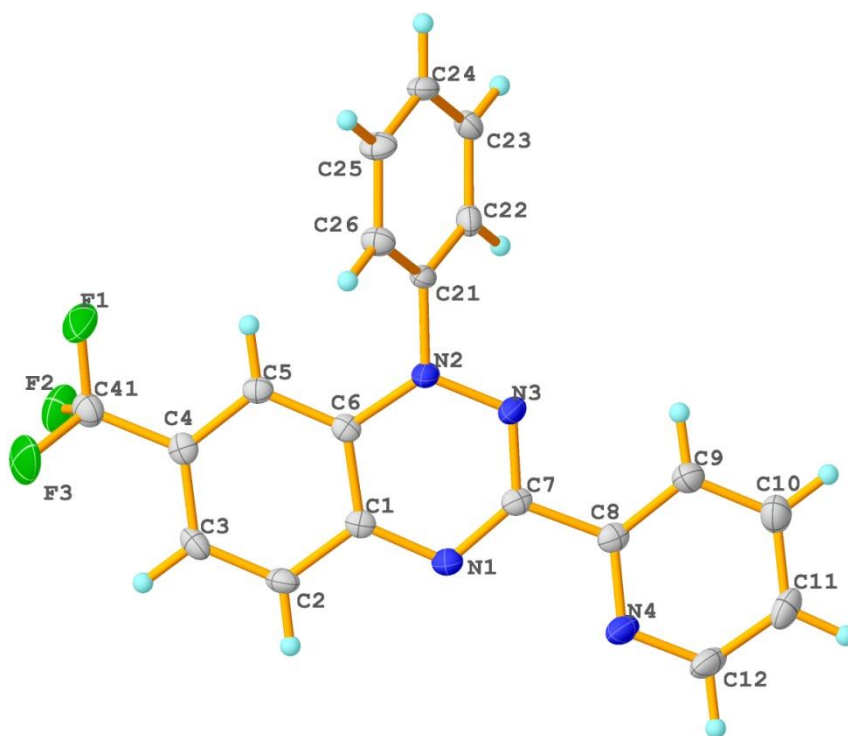
Figure S2. Molecular view of the benzotriazinyl radical **Rad₂** with atom numbering scheme.
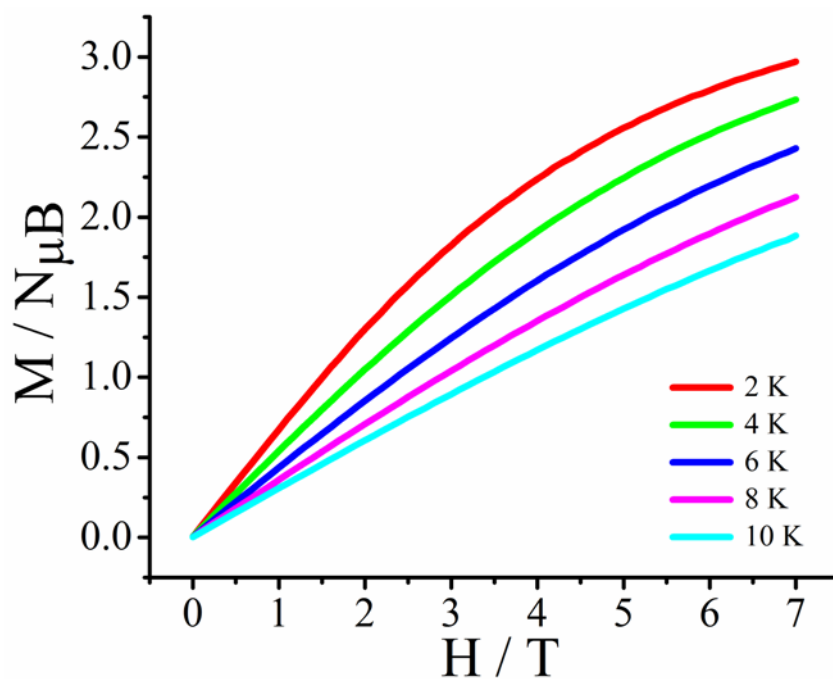
Figure S3. Field dependence of the magnetization of complex **2**.

Figure S4. Field dependence of the magnetization (circles) with simulations (solid lines) of complex **3**.

S.2 Computational results

To gain insight into the magnetic exchange coupling between the metal and radical ligand in **Rad$_2$**, complexes **1** and **2**, we performed density functional theory (DFT) calculations in combination with broken symmetry (BS) approach to obtain information on both metal-radical (J_a) and radical…radical (J_b) exchange couplings within the ORCA 4.0 software package. Calculations implemented the hybrid functional B3LYP with TZVP basis set for Zn and Ni and 6-311G* for other atoms. The tight SCF convergence criteria were employed throughout the calculation. For the S = ½ radical **Rad$_2$** and the zinc complex **1**, the exchange couplings via the π···π interaction between nearest-neighbour benzotriazinyl radicals (Figures 3 and 6b respectively in the main manuscript) were computed using the method of Yamaguchi where the exchange coupling is determined from the energies (E) and expectation values ($<S^2>$) of the triplet and broken symmetry singlet states:

$$J = \frac{-(E_T - E_{BSS})}{<S^2>_T - <S^2>_{BSS}}$$

Eq. 1

S.2.1 Benzotriazinyl radical, Rad$_2$

Radical Pair (J)	Energy (Hatree)	$<S^2>$
S = 1	-2498.364699	2.0319
S = 0 (BSS)	-2498.365114	1.0098

$J = -(E_T - E_{BSS}) / (<S^2_T> - <S^2_{BSS}>) = -89$ cm^{-1} (-128K)

4

Mulliken spin densities (in au) for high-spin (HS) and broken symmetry spin (BS) states of selected atoms in radical pair.

Selected Atoms	HS	BS
N2	0.275352	0.273063
N1	0.313052	0.308984
N3	0.273225	0.268679
N2	0.275336	-0.273048
N1	0.313075	-0.309007
N3	0.273188	-0.268645

S.2.2 [Zn(hfac)$_2$(Rad$_2$)] (1)

Zinc Complex Pair **1** (J_1)	Energy (Hatree)	$\langle S^2 \rangle$
S = 1	-9819.726231	2.0267
S = 0 (BSS)	-9819.726244	1.0265

$J = -(E_T - E_{BSS}) / (\langle S^2_T \rangle - \langle S^2_{BSS} \rangle) = -2.9$ cm^{-1} (-4.1 K)

Mulliken spin densities (in au) for high-spin (HS) and broken symmetry spin (BS) states of selected atoms in zinc complex pair **1**.

Selected Atoms	HS	BS
N4B	0.265352	0.263063
N2B	0.303052	0.298984
N3B	0.253225	0.248679
N4A	0.265336	-0.263048
N2A	0.303075	-0.299007
N3A	0.253188	-0.248645

Zinc Complex Pair **2** (J_2)	Energy (Hatree)	$\langle S^2 \rangle$
S = 1	-9819.748153	2.0253
S = 0 (BSS)	-9819.748169	1.0252

$J = -(E_T - E_{BSS}) / (\langle S^2_T \rangle - \langle S^2_{BSS} \rangle) = -3.5$ cm^{-1} (-5.1 K)

Mulliken spin densities (in au) for high-spin (HS) and broken symmetry spin (BS) states of selected atoms in zinc complex pair **2**.

Selected Atoms	HS	BS
N4B	0.285312	0.273093
N2B	0.323062	0.318984
N3B	0.263249	0.258879
N4A	0.285196	-0.273548
N2A	0.323045	-0.319177
N3A	0.263359	-0.258649

S.2.3 [Ni(hfac)$_2$(Rad$_2$)] (2)

To compute the intramolecular Ni$\cdots$**Rad$_2$** exchange coupling (J_a), the energies of the quartet and doublet states for an isolated molecule were calculated. To estimate the intermolecular exchange coupling between molecules of **2**, the Ni^{II} centres were replaced by diamagnetic Zn^{2+} and the energies of the triplet and broken symmetry singlet were computed.

Nickel Complex (J_a)	Energy (Hartree)	$\langle S^2 \rangle$
S = 3/2	-4638.971183	3.7703
S = ½	-4638.970127	1.7690

J_a = -(E$_Q$ – E$_D$)/($\langle S^2_Q \rangle$ – $\langle S^2_D \rangle$) = +116 cm^{-1} (+167 K)

Mulliken spin densities (in au) for high-spin (HS) and broken symmetry spin (BS) states of selected atoms in complex **2**.

Selected Atoms	HS	BS
Ni1B	1.663032	1.667250
N2B	0.345163	-0.230421
N3B	0.229371	-0.227010
N4B	0.276665	-0.282496

Nickel complex pair (J_b)	Energy (Hartree)	$\langle S^2 \rangle$
S = 1	-9820.012790	2.0270
S = 0	-9820.012804	1.0268

J_b = – (E$_T$ – E$_{BSS}$) / ($\langle S^2_T \rangle$ – $\langle S^2_{BSS} \rangle$) = -3.1 cm^{-1} (-4.4 K)

S.2.4 [Co(hfac)$_2$(Rad$_2$)] (3)

To compute the intramolecular Co$\cdots$**Rad$_2$** exchange coupling (J_a), the energies of the quartet and doublet states for an isolated molecule were calculated. To estimate the intermolecular exchange coupling between molecules of **3**, the Co^{II} centres were replaced by diamagnetic Zn^{2+} and the energies of the triplet and broken symmetry singlet were computed. The coupling constant was calculated using the method of Yamaguchi.

Cobalt Complex (J_a)	Energy (Hatree)	$\langle S^2 \rangle$
E_{HS}	-4513.140976	6.0265
E_{BS}	-4513.139979	3.0157

J_a = -(E_{HS} – E_{BS})/($\langle S^2_{HS} \rangle$ – $\langle S^2_{BS} \rangle$) = +72.7 cm^{-1} (+103.2 K)

Mulliken spin densities (in au) for high-spin (HS) and broken symmetry spin (BS) states of selected atoms in complex **3**.

Selected Atoms	HS	BS
Co1B	2.748497	2.741558
N2B	0.343363	-0.266019
N3B	0.260938	-0.261255
N4B	0.262319	-0.268731

Cobalt complex pair (J_b)	Energy (Hatree)	$<S^2>$
E_{HS}	-9819.754026	2.0264
E_{BS}	-9819.754038	1.0262

J_b = -(E_{HS} − E_{BS})/($<S^2_{HS}>$ − $<S^2_{BS}>$) = -3.1 cm^{-1} (-4.4 K)

S.2.4 .1 CASSCF calculation details for complex 3

The CASSCF/RASSI/Single_Aniso type calculations were performed by MOLCAS 8.2 software package.[1] In this calculation, all the atoms were described by ANO-RCC[2] basis set of function ([ANO-RCC-VTZP] for Co, [ANO-RCC-VTZ] for F, O, N and [ANO-RCC-VDZ] for C, H including relativistic effects by Douglas Kroll Hess Hamiltonian.[3] To save disk space, we employed the Cholesky decomposition for two electrons integral.[4] We have considered 7 electrons in 5 d-orbitals and 1 electron from the radical resulting in a CAS (8,6) active space for Co(II)-radical complex. All available spin states were optimized in these calculations, affording 15 quintets, 75 triplets and 90 singlets. These were mixed by spin-orbit coupling which was included by RASSI programme.[5] Additionally, the Single_Aniso module[6] has been used to compute the zero field splitting parameter and anisotropy of the low lying excited states. Alternatively, we have also performed the calculation with the reduced numbers of states (15 quintets, 40 triplets, and 30 singlets). However, no significant changes have been observed in the CASSCF result.

Single_Aniso computed parameters considering full spin states (15 quintets, 75 triplets and 90 singlets) and just a consideration of the lowest lying spin states (15 quintets, 40 triplets and 30 singlets) (in square brackets):

Complex	D (cm^{-1})	E (cm^{-1})	g_x, g_y, g_z
3	+33.7 [+33.12]	-4.5 [-4.32]	2.52, 2.36, 2.07 [2.51, 2.35, 2.09]

Reference:

1. F. Aquilante, L. De Vico, N. Ferre, G. Ghigo, P. -Å. Malmqvist, P. Neogrady, T. B. Pedersen, M. Pitonak, M. Reiher, B. O. Roos, L. Serrano-Andres, M. Urban, V. Veryazov and R. Lindh, *J. Comput. Chem.,* 2010, **31**, 224–247.

2. B. O. Roos, R. Lindh, P.-Å. Malmqvist, V. Veryazov, P.-O. Widmark and A. C. Borin, *J. Phys. Chem. A*, 2008, **112**, 11431-11435.

3. a) M. Douglas and N. M. Kroll, *Ann. Phys.*, 1974, **82**, 89-155; b) B. A. Hess, *Phys. Rev. A*, 1986, **33**, 3742-3748. c) M. Reiher, *WIREs Comput. Mol. Sci.*, 2012, **2**, 139-149; d) F. Aquilante, P.-Å. Malmqvist, T. B. Pedersen, A. Ghosh and B. O. Roos, *J. Chem. Theory Comput.*, 2008, **4**, 694-702.

4. F. Aquilante, P.-Å. Malmqvist, T. B. Pedersen, A. Ghosh and B. O. Roos, *J. Chem. Theory Comput.,* 2008, **4**, 694-702.

5. P. Å. Malmqvist, B. O. Roos and B. Schimmelpfennig, *Chem. Phys. Lett.*, 2002, **357**, 230-240.

6. L. F. Chibotaru and L. Ungur, *J. Chem. Phys.*, 2012, **137**, 064112.

Table S1. Crystallographic data and structure refinement for **Rad$_2$** and M(hfac)$_2$(**Rad$_2$**) (M = Zn(II) (**1**), Ni(II) (**2**) and Co(II) (**3**), hfac: hexafluoroacetylacetonate)

Identification code	Rad$_2$	1	2	3
Empirical formula	C$_{19}$H$_{12}$F$_3$N$_4$	C$_{29}$H$_{14}$F$_{15}$N$_4$O$_4$Zn	C$_{29}$H$_{14}$F$_{15}$N$_4$O$_4$Ni	C$_{29}$H$_{14}$F$_{15}$N$_4$O$_4$Co
Formula weight	353.33	832.81	826.15	826.37
Temperature/K	140.01	140.01	140.01	140.01
Crystal system	triclinic	monoclinic	monoclinic	monoclinic
Space group	*P*-1	*P*2$_1$/n	*P*2$_1$/n	*P*2$_1$/n
a/Å	7.5072(5)	13.7227(8)	13.6466(19)	13.7407(11)
b/Å	10.1625(5)	23.2862(14)	23.027(4)	23.4881(18)
c/Å	11.5906(8)	20.7274(11)	21.015(3)	21.1641(17)
α/°	70.372(3)	90	90	90
β/°	79.685(3)	105.370(3)	105.376(5)	105.500(4)
γ/°	71.518(3)	90	90	90
Volume/Å^3	787.32(9)	6386.5(6)	6367.3(16)	6582.1(9)
Z	2	8	8	8
ρ_{calc}g/cm^3	1.490	1.732	1.724	1.668
μ/mm^{-1}	0.117	0.900	0.740	0.648
F(000)	362.0	3304.0	3288.0	3280.0
Crystal size/mm^3	0.5 × 0.04 × 0.03	0.70 × 0.30 × 0.10	0.50 × 0.05 × 0.05	0.30 × 0.02 × 0.02
Radiation	MoKα (λ = 0.71073)	MoKα (λ = 0.71073)	MoKα (λ = 0.71073)	MoKα (λ = 0.71073)
2θ range for data collection/°	4.87 to 51.998	3.54 to 49.998	4.478 to 51.364	3.188 to 52.096
Index ranges	-9 ≤ h ≤ 9, -12 ≤ k ≤ 12, -14 ≤ l ≤ 14	-16 ≤ h ≤ 15, -27 ≤ k ≤ 27, -22 ≤ l ≤ 24	-16 ≤ h ≤ 16, -28 ≤ k ≤ 28, -25 ≤ l ≤ 25	-16 ≤ h ≤ 16, -26 ≤ k ≤ 28, -26 ≤ l ≤ 23
Reflections collected	13228	11233	108167	51858
Independent reflections	3094 [R$_{int}$ = 0.0591, R$_{sigma}$ = 0.0450]	11233 [R$_{int}$ = -, R$_{sigma}$ = 0.0621]	12093 [R$_{int}$ = 0.1293, R$_{sigma}$ = 0.0814]	12794 [R$_{int}$ = 0.0694, R$_{sigma}$ = 0.0923]
Data/restraints/parameters	3094/0/235	11233/224/1055	12093/213/1090	12794/195/1054
Goodness-of-fit on F^2	1.044	1.038	1.028	1.045
Final R indexes [I≥ 2σ (I)]	R$_1$ = 0.0454, wR$_2$ = 0.1009	R$_1$ = 0.0707, wR$_2$ = 0.1760	R$_1$ = 0.0602, wR$_2$ = 0.0966	R$_1$ = 0.0829, wR$_2$ = 0.2291
Final R indexes [all data]	R$_1$ = 0.0743, wR$_2$ = 0.1143	R$_1$ = 0.1137, wR$_2$ = 0.2026	R$_1$ = 0.1220, wR$_2$ = 0.1150	R$_1$ = 0.1783, wR$_2$ = 0.2789
Largest diff. peak/hole/e Å^{-3}	0.21/-0.32	0.85/-0.70	0.54/-0.47	0.77/-0.54